Journal of Dermatological Science 62 (2011) 183–191

Contents lists available at ScienceDirect

Journal of Dermatological Science

journal homepage: www.elsevier.com/jds

Imatinib mesylate induction of ROS-dependent apoptosis in melanoma B16F0 cells

Shao-Ping Chang [a,b,c], Shing-Chuan Shen [d], Woan-Rouh Lee [a,d,e], Ling-Ling Yang [f], Yen-Chou Chen [d,g,*]

[a] Graduate Institute of Clinical Medicine, College of Medicine, Taipei Medical University, Taipei, Taiwan
[b] Department of Cosmetic Dermatology, Shin Kong Wu Ho-Su Memorial Hospital, Taipei, Taiwan
[c] Department of Dermatology, China Medical University Hospital, Taipei Branch, Taipei, Taiwan
[d] Graduate Institute of Medical Sciences, College of Medicine,Taipei Medical University, Taipei, Taiwan
[e] Department of Dermatology, Taipei Medical University-Shuang Ho Hospital, New Taipei City, Taiwan
[f] Graduate Institute of Pharmacognosy, Taipei Medical University, Taipei, Taiwan
[g] Cancer Research Center and Orthopedics Research Center, Taipei Medical University Hospital, Taipei, Taiwan

ARTICLE INFO

Article history:
Received 12 October 2010
Received in revised form 15 February 2011
Accepted 8 March 2011

Keywords:
Imatinib mesylate (STI571)
Reactive oxygen species
MAPKs
Apoptosis
Melanoma cells

ABSTRACT

Background: Imatinib mesylate (STI571), a protein tyrosine kinase inhibitor, was shown to reduce the viability of several cancer cell lines via apoptosis induction; however, the role of reactive oxygen species (ROS) in STI571-induced melanoma cell apoptosis is still undefined.
Objective: In this study, we investigated the contribution of ROS to STI571-induced apoptosis in melanoma B16F0 cells, and the apoptotic mechanism elicited by STI571 was illustrated.
Methods: Using an in vitro cell culture system, the effects of STI571 on ROS production, cell cycle progression, caspase activation, and mitochondrial functions were examined via Western blotting, a flow cytometric analysis, an enzyme activity assay, and a DNA integrity assay. In pharmacological studies, the ROS scavenger, N-acetyl cysteine (NAC), the NADPH oxidase inhibitor, dipheylene iodide (DPI), and mitogen-activated protein kinase (MAPK) inhibitors (PD98059, SP600125, and SB203580) were applied to investigate the mechanism.
Results: STI571 reduced the viability of melanoma cells B16F0, but not human skin fibroblasts WS1, via apoptosis induction. Besides, apoptosis induced by STI571 was inhibited by the addition of NAC and DPI, and an increase in the intracellular peroxide level by STI571 was identified in melanoma B16F0 cells. Activation of caspases 3 and 9 enzyme activities accompanied by disrupting the mitochondria membrane potential in according with stimulating JNK and p38 protein phosphorylation was identified in STI571-treated B16F0 cells. STI571-mediated a ROS-dependent apoptosis potentiated by JNK inhibitor SP600125 was first identified in melanoma B16F0 cells.
Conclusion: Our results support the idea that ROS-dependent apoptosis in STI571-treated melanoma cells B16F0. The combination of a JNK inhibitor with STI571 for treating melanomas is suggested for further in vivo studies.

1. Introduction

Melanomas are usually resistant to chemotherapy and radiation therapy; therefore, surgery remains the major treatment in clinical practice. Previous studies showed that the resistance of melanoma cells to apoptosis induction is conferred by activation of survival signaling pathways. The mitogen-activated protein kinase (MAPK) pathway is constitutively activated in melanomas, and has received the most attention in developing therapies for melanomas [1]. Therefore, agents in combination with MAPK inhibitors are critical in treating melanomas, and deserve further investigation [2,3].

Induction of apoptosis through the mitochondrial pathway is a strategy for treating melanomas [4]. Alternative activations of

Abbreviations: Bcl-2, B-cell lymphoma 2; Cyt c, cytochrome c; DCFH-DA, 2′,7′-dichlorofluorescein diacetate; DMSO, dimethyl sulfoxide; DPI, dipheylene iodide; ERK, extracellular regulated kinase; JNK, c-Jun-N-terminal protein kinase; MAPK, mitogen-activated protein kinase; MTT, tetrazolium dye 3-(4,5,-dimethylthiazol)-2-yl-2,5-diphenyltetrazolium bromide; NAC, N-acetyl cysteine; NADPH, nicotinamide adenine dinucleotide phosphate; ROS, reactive oxygen species; Cyc B1, cyclin B1; Cyc D2, cyclin D2; STI571, imatinib mesylate.

* Corresponding author at: Graduate Institute of Medical Sciences, College of Medicine, Taipei Medical University, Taipei, Taiwan. Tel.: +886 2 27361661x3421; fax: +886 2 23787139.
E-mail address: yc3270@tmu.edu.tw (Y.-C. Chen).

0923-1811/$36.00 © 2011 Japanese Society for Investigative Dermatology. Published by Elsevier Ireland Ltd. All rights reserved.
doi:10.1016/j.jdermsci.2011.03.001

Bcl-2 family proteins, including anti- and pro-apoptotic proteins, participate in the apoptotic mitochondrial pathway. Decreases in anti-apoptotic proteins such as Bcl-2 or increases in pro-apoptotic proteins promote the release of cytosolic cytochrome (Cyt) c from mitochondria to activate caspases 9 and 3, and induce apoptosis [5,6]. Reactive oxygen species (ROS) are important in tumor cell apoptosis, mitochondrial stability, and chemotherapeutic effects [7–9]. Elevated ROS production was identified in apoptosis induced by various anticancer drugs such as taxol, cisplatin, and doxorubin [10–12]. However, ROS may act as mitogens to stimulate the proliferation and migration of tumor cells [13,14]. Previous studies showed that ROS in melanoma cells are abundant due to melanin metabolism, and they contribute to DNA damage and activation of proto-oncogenes [15]. Therefore, more evidence is needed to verify the role of ROS generators in treating melanomas.

Imatinib mesylate (STI, Gleevec, STI571) is the first small-molecular drug used as targeted therapy which initially focused on the tyrosine kinase receptors such as c-KIT, platelet-derived growth factor (PDGF) α and β and Abl-Bcr [16]. STI571 inhibits activation of these tyrosine kinase receptors through blocking ATP-binding sites and is accepted as the first-line treatment for chronic myelogenic leukemia and gastrointestinal stromal tumors [17–19]. Although many biological actions of STI571 were reported such as improvement of chemotherapeutic drug penetration, down-regulation of telomerase activity, the roles of ROS and the apoptotic mitochondrial pathway in STI571-treated melanoma cells apoptosis are still undefined [20,21]. The aim of this study was to investigate the apoptotic mechanism of STI571 in melanoma cells B16F0, and to elucidate the roles of ROS and MAPKs in STI571-induced apoptosis.

2. Materials and methods

2.1. Chemicals and reagents

STI571 and nilotinib were kindly provided by Novartis Pharmaceuticals (Basel, Switzerland). N-Acetyl cysteine and diphenyleneiodonium (DPI) were from Sigma (St. Louis, MO). Antibodies against Bcl-2, total-JNK, ERK, and p38 (at a 1:1000 dilution) were from Santa Cruz Biotechnology (Santa Cruz, CA). Antibodies against pro-PARP, phospho-specific AKT (Ser473/Thr308), ERK (Thr202/Tyr204), JNK (Thr183/Tyr185), p38, and total-AKT (at 1:1000 dilutions) were purchased from Cell Signaling Technology (Danvers, MA). The anti-α-tubulin and Cyt c antibodies were from Neomarker (Fremont, CA). SB203580 and SP600125 were purchased from Calbiochem (La Jolla, CA). D4-GDI, and caspases 3 and 9 were purchased from Imgenex (San Diego, CA) Ten-millimolar DPI stock solutions were prepared in dimethyl sulfoxide (DMSO, Sigma). DPI was diluted in culture medium to treat cells. DMSO (0.01%) diluted in the medium was used as the vehicle control.

2.2. Cell culture

Murine melanoma B16F0 cells and normal human embryonic skin fibroblasts WS1 were grown in Dulbecco's modified Eagle's medium (Invitrogen, Carlsbad, CA) supplemented with 10% fetal bovine serum (Hyclone, Logan, UT), 5 U/ml penicillin, 5 μg/ml streptomycin, and 200 mM L-glutamine at 37 °C in a 5% CO_2 atmosphere.

2.3. MTT assay

Proliferation of cultured cells seeded into 24-well uncoated plastic plates (Costar) at 50,000 cells/well (except where indicated) was quantitated as previously described using a colorimetric method based on the metabolic reduction of the soluble yellow tetrazolium dye, 3-(4,5-dimethylthiazol)-2-yl-2,5-diphenyltetrazolium bromide (MTT), to the insoluble purple formazan by the action of mitochondrial succinyl dehydrogenase [22]. B16F0 cells were then incubated at 37 °C for 4 h under 5% CO_2/95% air, followed by dissolution in 500 μl of a lysis solution (10% sodium dodecylsulfate (SDS) in 0.01 N HCl). The absorbance of the solution was read at 595 nm using a multiplate reader, and cell viability was expressed as the OD_{595} of treated cells.

2.4. LDH release assay

The percentage of LDH release from B16F0 cells under indicated treatments was detected using cytotoxicity detection kit (Roche, Indianapolis, IN, USA), The activity was monitored as the oxidation of the reduced form of nicotinamide-adenine dinucleotide (NADH) at 530 nm, and cytotoxicity was determined by the equation: [(OD530 of the treated group − OD530 of the control group)/(OD530 of the Triton X-100-treated group − OD530 of the control group)] × 100%.

2.5. Detection of chromatin-condensed cells

B16F0 cells after different treatments were fixed by cold methanol followed by adding 10% Giemsa solution for 30 min. Then, the extracellular dye was removed by PBS addition for several times. The chromatin condensed cells were observed microscopically.

2.6. Measurement of ROS generation by intact cells

Intracellular production of ROS by B16F0 melanoma cells was measured by oxidation of DCFH-DA to DCF. DCFH-DA is a non-polar compound that readily diffuses into cells, where it is hydrolyzed to the non-fluorescent polar derivative, DCFH, and thereby trapped within cells. If DCFH-DA is oxidized, it turns into the highly fluorescent DCF. B16F0 cells were incubated in the dark for 10 min at 37 °C with 50 μM DCFH-DA, then harvested, and resuspended in plain medium. The fluorescence was analyzed using a FACScan (Becton Dickinson, Sunnyvale, CA) flow cytometer with excitation at 488 nm and emission at 530 nm.

2.7. Western blot analysis

Cells lysates were prepared by suspending cells in lysis buffer (50 mM Tris–HCl (pH 7.4), 1% Nonidet P-40, 150 mM NaCl, 1 mM EGTA, 0.025% sodium deoxycholate, 1 mM sodium fluoride, 1 mM sodium orthovanadate, and 1 mM phenylmethylsulfonyl fluoride). Protein samples (30 μg) were electrophoresed on a 8%, 10%, or 13% SDS-polyacrylamide gels, and transferred to polyvinylidene difluoride (PVDF) membranes (Millipore, Bedford, MA). The membrane was blocked with 1% bovine serum albumin (BSA) at room temperature for 1 h and then incubated with specific antibodies (pro-PARP, D4-GDI, caspases 3 and 9, BCL-2, Cyt c, Cyc B1 and D2, Cdc 2, phosphorylated AKT, JNK and p38, and total AKT, JNK, and p38) as indicated for a further 3 h. Protein expression was quantified by incubation with the colorimetric substrates, nitro blue tetrazolium (NBT; Roth, Karlsruhe, Germany) and 5-bromo-4-chloro-3-indolyl-phosphate (BCIP).

2.8. DNA fragmentation assay

B16F0 cells under different treatments were collected, and then lysed in 100 μl of lysis buffer (50 mM Tris, pH 8.0; 10 mM ethylenediaminetetraacetic acid (EDTA); 0.5% sodium sarkosinate,

and 1 mg/ml proteinase K) for 3 h at 56 °C. Then, 0.5 mg/ml RNase A was added to each reaction for another hour at 56 °C. DNA was extracted with phenol/chloroform/isoamyl alcohol (25/24/1) before loading. Samples were mixed with loading buffer (50 mM Tris, 10 mM EDTA, 0.025% (w/w) bromophenol blue), and loaded onto a pre-solidified 2% agarose gel containing 0.1 mg/ml ethidium bromide. The agarose gels were run at 100 V for 45 min in TBE buffer, then observed and photographed under UV light.

2.9. Measurement of mitochondrial membrane potential

After indicated treatments, B16F0 cells were incubated with 40 nM DiOC6(3) for 15 min at 37 °C, and cells were washed with ice-cold PBS and collected by centrifugation at 500 × *g* for 10 min. The pellets were then resuspended in 500 ml of PBS, and fluorescence intensities of DiOC6(3) were analyzed on a flow cytometer (FACScan, Becton Dickinson, San Jose, CA) with excitation and emission settings of 484 and 500 nm, respectively.

2.10. Measurement of hypodiploid cells ratio via PI staining

B16F0 cells under different treatments were washed with ice-cold PBS, and fixed in 70% ethanol at-20 °C for at least 1 h. After fixation, cells were washed twice, incubated in 0.5 ml of 0.5% Triton X-100/PBS at 37 °C for 30 min containing 1 mg/ml of RNase A, and stained with 0.5 ml of 50 mg/ml propidium iodide for an

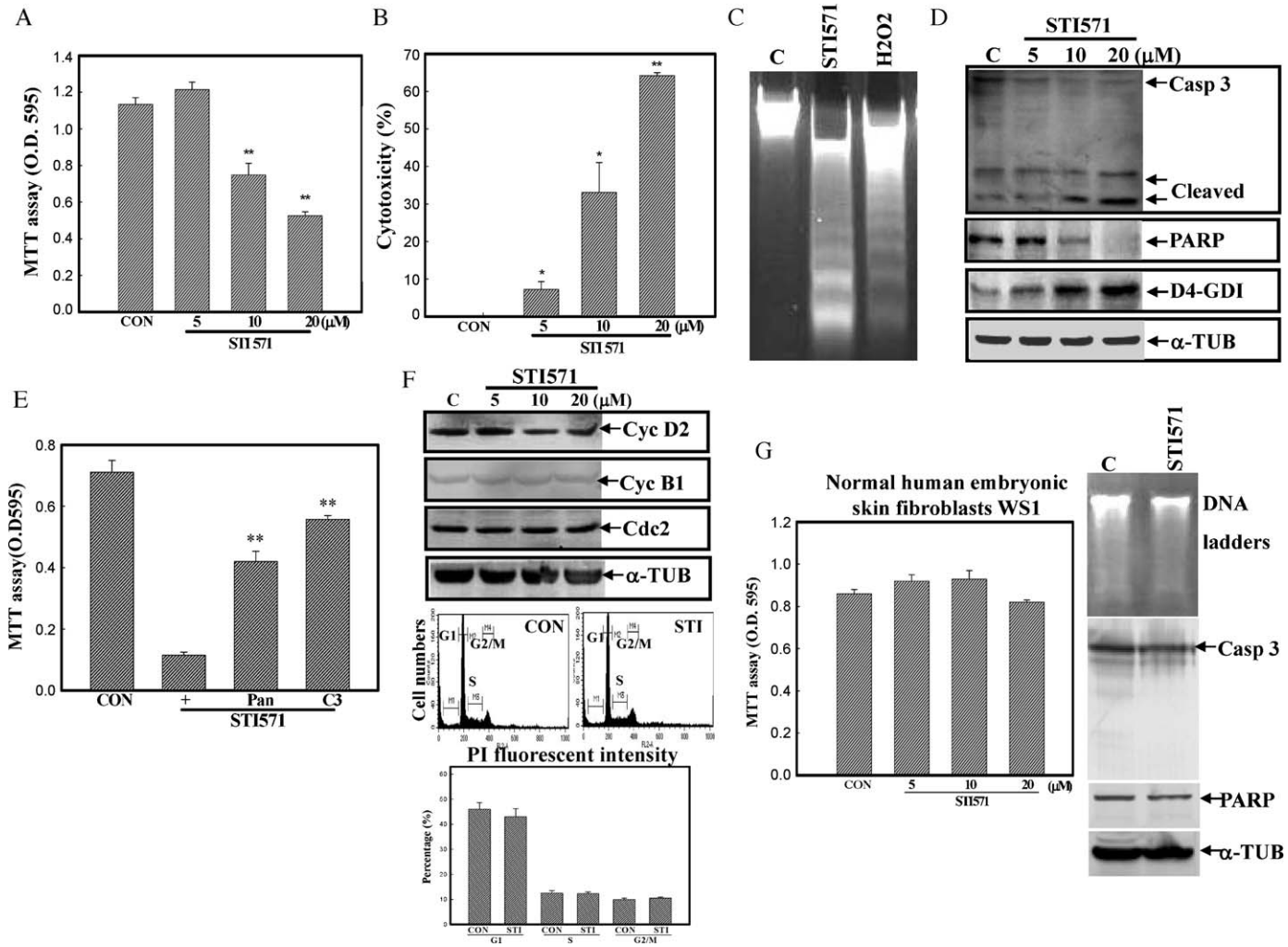

Fig. 1. STI571 reduction of viability through apoptosis induction in melanoma B16F0 cells. (A) The viability of B16F0 cells under STI571 treatment was examined by an MTT assay. Cells were treated with different concentrations (5, 10, and 20 μM) of STI571 for 24 h, and the viability of cells was examined by an MTT assay. (B) Cytotoxicity of STI571 in B16F0 cells was detected by an LDH-release assay. As described in (A), the amount of LDH in the medium was measured by an LDH detection kit, and the cytotoxicity was examined as described in "Section 2". (C) Induction of DNA ladders by STI571 in B16F0 cells. As described in (A), the integrity of DNA in STI571 (20 μM) or H_2O_2 (100 μM)-treated B16F0 cells was analyzed. DNA ladders induced by H_2O_2 were described as a positive control. (D) Induction of caspase 3 (Casp 3), PARP, and D4-GDI protein cleavage by STI571. As described in (A), expressions of cleaved caspase 3 (Casp 3), PARP, and the cleaved D4-GDI protein were examined by Western blotting using specific antibodies. α-Tubulin (α-TUB) protein was used as an internal control to verify that equal amounts of proteins were loaded in each lane. (E) The caspase inhibitors, VAD-FMK (Pan; 50 μM) and DEVD-FMK (C3; 50 μM), protected B16F0 cells from STI571 (20 μM)-induced cell death. Cells were treated with the indicated inhibitors for 1 h followed by STI571 (20 μM) for an additional 24 h. Viability of cells under different treatments was evaluated by an MTT assay. (F) Effects of STI571 on cell cycle progression and cell cycle regulator proteins cyclin D2, B1, and cdc2 expression in melanoma cells B16F0 were examined by flow cytometric analysis and Western blotting. (Upper panel) In Western blotting, cells were treated with different concentrations of STI571 for 24 h, and expression of indicated proteins was examined. (Lower panel) cells were treated with vehicle (CON) or STI571 (STI; 20 μM) for 24 h, and ratio of G1, S, and G2/M was measured by flow cytometry analysis using PI staining. Data are expressed as the mean ± SE from three independent experiments by Student's *t*-test. (G) Effects of STI571 on the viability, DNA integrity, and apoptotic proteins caspase 3 and PARP expression in normal embryonic skin fibroblasts WS1. (Left panel) WS1 cells were treated with different concentrations of STI571 for 24 h, and viability of cells was analyzed by MTT assay. (Right panel) WS1 cells were treated with vehicle (CON) or STI571 (20 μM) for 24 h, and DNA integrity and expression of caspase 3, PARP, and α-TUB protein were examined. Data are expressed as the mean ± SE from three independent experiments. $^{*}p < 0.05$ and $^{**}p < 0.01$ denote a significant difference compared to the vehicle (CON) group (A and B) or the STI571-treated group (E) by Student's *t*-test. Data of Western blotting and DNA ladders have been repeated independently at least three times, and similar results were obtained.

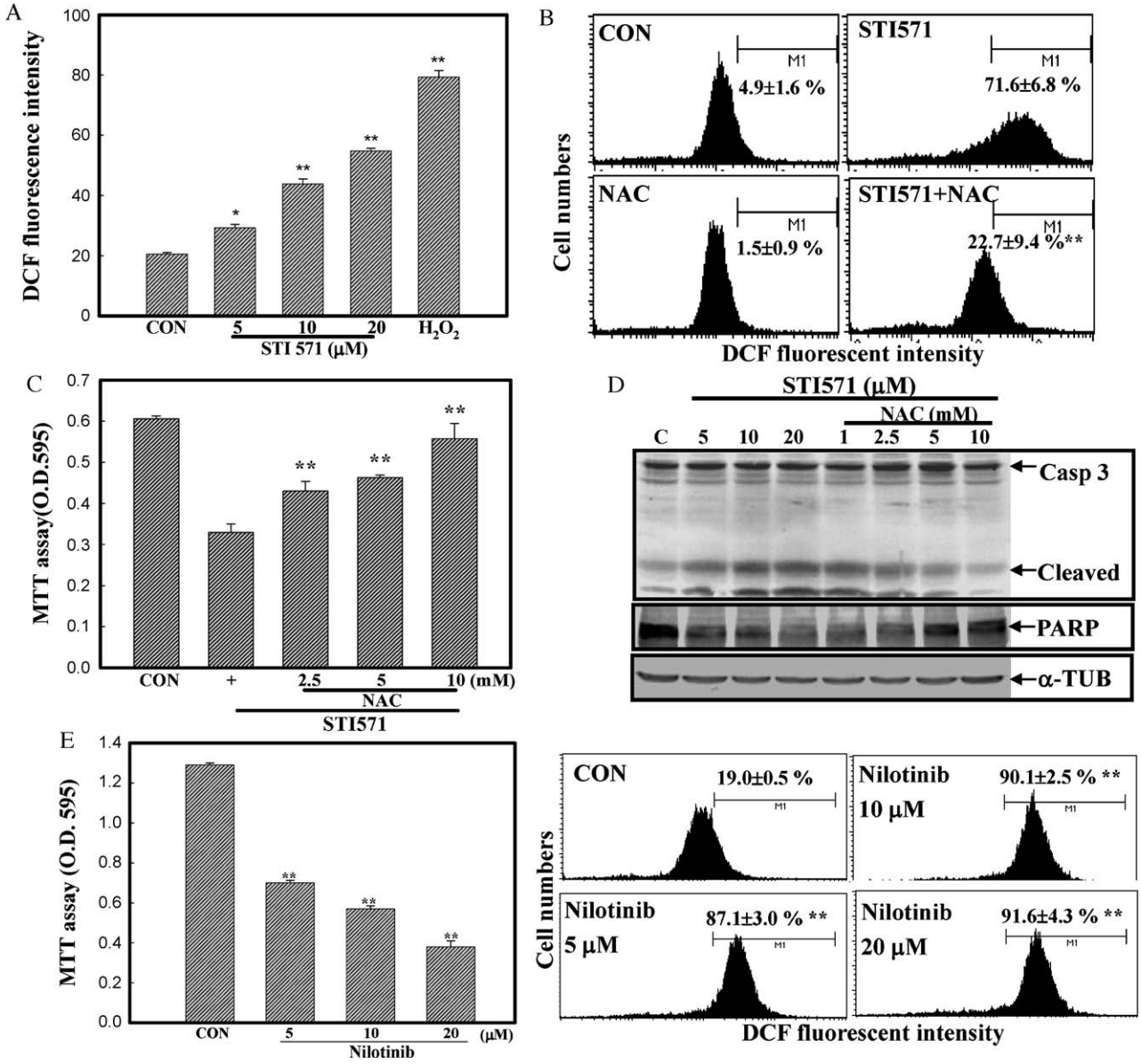

Fig. 2. ROS production in STI571-induced cell death. (A) An increase in intracellular peroxide production in STI571-treated B16F0 cells by a flow cytometric analysis using DCHF-DA as a fluorescent dye. Cells were treated with different concentrations (5, 10, and 20 μM) of STI571 for 2 h followed by the addition of DCHF-DA (100 nM) for 30 min. The fluorescent intensity of DCF in cells under different treatments was detected by a flow cytometric analysis. (B) NAC treatment inhibited STI571-induced peroxide production by B16F0 cells. Cells were treated with NAC for 30 min followed by STI571 (20 μM) treatment for 2 h for the DCHF-DA assay. (C) NAC prevention of B16F0 cells from STI571-induced cell death by an MTT assay. As described in (B), viability of cells after STI571 stimulation for 24 h was analyzed by an MTT assay. (D) NAC inhibition of STI571-induced caspase 3 and PARP protein cleavage in B 16 cells. As described in (C), expressions of caspase 3, PARP, and α-TUB proteins were detected by Western blotting using specific antibodies. (E) Nilotinib induction of cytotoxic effect against the viability of melanoma cells B16 with inducing intracellular peroxide production. (Left panel) B16 cells were treated with different concentrations (5, 10, and 20 μM) of nilotinib for 24 h followed by MTT assay for viability detection. (Right panel) Cells were treated with different concentrations (5, 10, and 20 μM) of nilotinib for 2 h followed by the addition of DCHF-DA (100 nM) for 30 min. The fluorescent intensity of DCF in cells under different treatments was detected by a flow cytometric analysis. Data are expressed as the mean ± SE from three independent experiments. $^{*}p < 0.05$ and $^{**}p < 0.01$ denote a significant difference compared to the vehicle (CON) group (A and E) or the STI571-treated group (B and C) by Student's *t*-test. Data of Western blotting have been repeated independently at least three times, and similar results were obtained.

additional 10 min. The fluorescence emitted from the propidium–DNA complex was quantitated after excitation of the fluorescent dye by FACScan flow cytometry (Becton Dickenson).

2.11. Statistical analysis

Values in the present study are expressed as the mean ± S.E. The significance of the difference from the respective groups in each experimental test condition was assayed using Student's *t*-test for each paired experiment. A *p*-value of <0.01 or <0.05 was regarded as indicating a significant difference.

3. Results

3.1. STI571 reduction of cellular viability via apoptosis induction in melanoma B16F0 cells

First, the effect of STI571 on the viability of melanoma B16F0 cells was examined by MTT and LDH-release assays. As illustrated in Fig. 1A, data of the MTT assay showed that STI571 concentration-dependently inhibited the viability in melanoma B16F0 cells, and the IC_{50} value of STI571 was 18.7 ± 0.8 μM. In the same part of the experiment, data of the LDH-release assay indicated that a

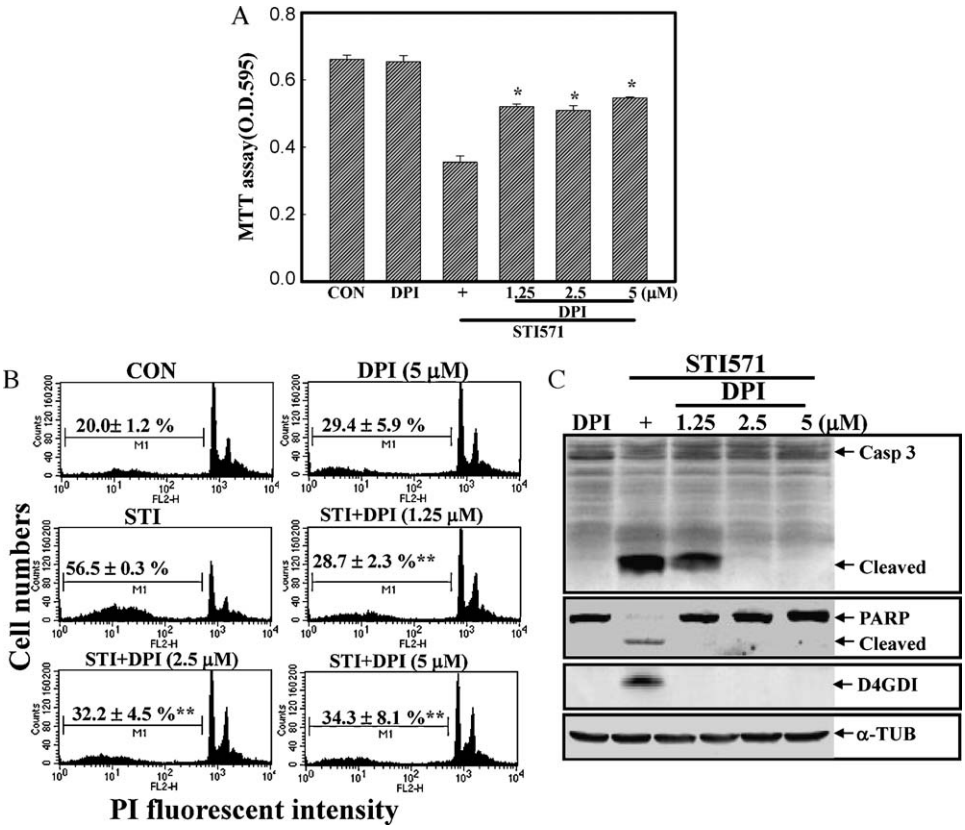

Fig. 3. DPI inhibition of STI571-induced ROS production and cell death in B16F0 cells. (A) DPI protection of B16F0 cells from STI571 (20 μM)-induced cell death. Cells were treated with different concentrations (1.25, 2.5, and 5 μM) of DPI for 30 min followed by STI571 stimulation, and the viability of cells was examined by an MTT assay. (B) DPI inhibition of STI571-induced hypodiploid cells in B16F0 cells. As described in (A), the ratio of hypodiploid cells under different treatments was examined by a flow cytometric analysis using PI staining. (C) DPI inhibition of STI571-induced caspase 3, PARP, and D4-GDI protein cleavage in B16F0 cells. As described in (A), expressions of caspase 3, PARP, D4-GDI, and a-tubulin proteins in B16F0 cells under STI571 stimulation were examined by Western blotting using specific antibodies. Data are expressed as the mean ± SE from three independent experiments. $^{*}p < 0.05$ and $^{**}p < 0.01$ denote a significant difference compared to the STI571-treated group by Student's *t*-test. Data of Western blotting had been repeated independently at least three times, and similar results were obtained.

concentration-dependent increase in cytotoxicity was elicited by STI571 (Fig. 1B). Investigation of DNA integrity in B16F0 cells under STI571 treatment showed that there were increased DNA ladders in STI571-treated B16F0 cells (Fig. 1C). Furthermore, STI571 induction of caspase 3 and the downstream PARP (115 kDa; precursor form) and D4-GDI (23 kDa; cleaved form) proteins were detected in B16F0 cells via Western blotting using specific antibodies (Fig. 1D). Increases in cleaved caspase 3 and D4-GDI proteins, and a decrease in PARP protein in B16F0 cells were found with STI571 treatment. Application of the caspase 3 inhibitor, DEVD-FMK (C3), or the pan-caspase inhibitor VAD-FMK (Pan) significantly protected B16F0 cells from STI571-induced cell death according to the MTT assay (Fig. 1E). Analysis of cell cycle progression showed that no alternation in the ratio of B16F0 cells at G1, S, and G2/M phase under STI571 stimulation via flow cytometry analysis using PI staining. As the same part of experiment, protein levels of cyclin D2, B1, and cdc2 were not changed by STI571 in B16F0 cells via Western blotting using specific antibodies (Fig. 1F). Additionally, effects of STI571 on normal human embryonic skin fibroblasts WS1 were examined, and data as shown in Fig. 1G. It indicated that STI571 did not affect the viability of WS1 cells and there was no alternation in DNA integrity, PARP and caspase 3 protein expression of WS1 cells (Fig. 1G).

3.2. Elevation of intracellular peroxide levels by STI571 in melanoma B16F0 cells

DCHF-DA, a peroxide-sensitive fluorescent substrate, was used in this study to examine the effects of STI571 on ROS production in melanoma B16F0 cells. As illustrated in Fig. 2A, an increase in intracellular peroxide was seen in STI571 (20 μM)-treated B16F0 cells, as characterized by an increase in the DCF fluorescent intensity in cells, and it was significantly inhibited by the addition of NAC (Fig. 2B). Data of peroxide production stimulated by H_2O_2 and inhibited by NAC were used as a positive control. Additionally, NAC addition significantly protected B16F0 cells from STI571-induced cell death according to the MTT assay (Fig. 2C). Data of Western blotting showed that STI571-induced caspase 3 and PARP protein cleavage was blocked by the addition of NAC to B16F0 cells (Fig. 2D). Additionally, the effect of a STI571-related compound nilotinib on ROS production and viability of B16F0 cells was examined, and nilotinib exhibited a concentration-dependent cytotoxic effect against the viability of B16F0 cells in accord with increased intracellular peroxide production (Fig. 2E). Involvement of ROS production in STI571/nilotinib-induced cell death was thus illustrated.

3.3. The NADPH oxidase inhibitor, DPI, protects B16F0 cells from STI571-induced apoptosis in B16F0 cells

Because NADPH oxidase is an important enzyme in ROS production, we further investigated if NADPH oxidase participates in STI571-induced cell death. Data of Fig. 3A show that incubation of B16F0 cells with the NADPH oxidase inhibitor, DPI, significantly inhibited STI571-induced cell death in B16F0 cells. The hypodiploid cell ratio in B16F0 cells treated with STI571 in the presence or absence DPI was examined using a flow cytometric analysis.

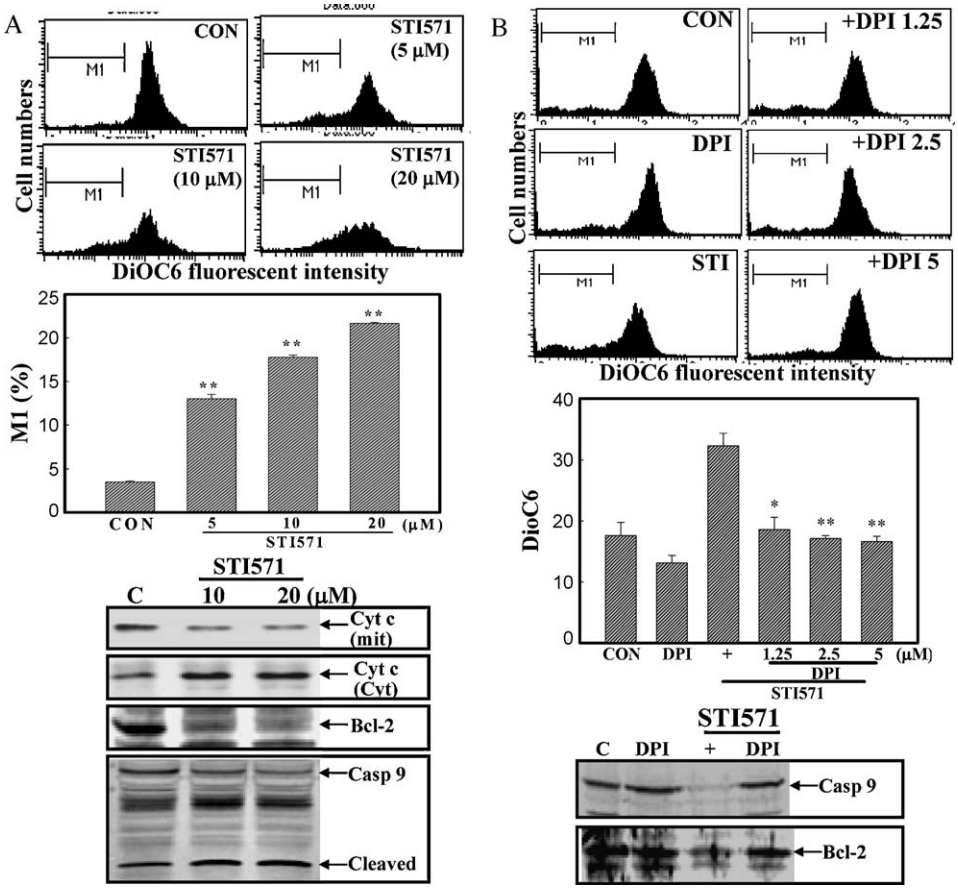

Fig. 4. Loss of mitochondrial membrane potential in B16F0 cells by STI571. (A) STI571 disrupted the mitochondrial membrane potential in accordance with increased cytochrome (Cyt) c and caspase 9 protein cleavage, and decreased Bcl-2 protein in B16F0 cells. (Upper panel) Cells were treated with different concentrations of STI571 for 24 h, and the mitochondrial membrane potential was examined by a flow cytometric analysis using $DiOC_6$ as a fluorescent dye. (Lower panel) As described before, expressions of mitochondria (mit) and Cyt c, and Bcl-2 and caspase 9 proteins were examined by Western blotting as described in "Section 2". (B) DPI protected B16F0 cells from STI571-induced reduction in the mitochondrial membrane potential, and decreases in caspase 9 and Bcl-2 protein. Cells were treated with different concentrations of DPI for 30 min followed by STI571 stimulation for 24 h. (Upper panel) The mitochondrial membrane potential was examined by a flow cytometric analysis using $DiOC_6$ as a mitochondrial fluorescent dye. (Lower panel) The expression caspase 9 and Bcl-2 proteins in cells was examined by Western blotting. Data are expressed as the mean ± SE from three independent experiments. $^{*}p < 0.05$ and $^{**}p < 0.01$ denote a significant difference compared to the vehicle (CON) group (A) or the STI571-treated group (B) by Student's *t*-test. Data of Western blotting have been repeated independently at least three times, and similar results were obtained.

Results indicated that DPI addition significantly decreased the STI571-induced hypodiploid cell ratio in B16F0 cells (Fig. 3B). Increased caspase 3, PARP, and D4-GDI protein cleavage by STI571 was blocked by the addition of DPI (Fig. 3C). This indicates that NADPH oxidase may contribute to STI571-induced apoptosis in melanoma B16F0 cells.

3.4. ROS-dependent decreases in the mitochondria membrane potential by STI571

The mitochondrial transmembrane potential ($\Delta\psi m$) in STI571-treated B16F0 cells was determined by a flow cytometric analysis using DiOC6 as a mitochondrion-sensitive fluorescent dye. STI571 induced a concentration-dependent decrease in the mitochondrial membrane potential in melanoma B16F0 cells (Fig. 4A, upper panel). Translocation of mitochondrial Cyt c to the cytosol was identified in STI571-treated B16F0 cells with decreased Bcl-2 protein and increased caspase 9 protein cleavage, characterized by a reduced level of caspase 9 protein (Fig. 4A, lower panel). In the presence of DPI treatment, STI571's disruption of the mitochondrial membrane potential was significantly prevented in B16F0 cells (Fig. 4B, upper panel). Additionally, STI571-induced decreases in Bcl-2 and caspase 9 proteins were blocked by the addition of DPI (Fig. 4B, lower panel).

3.5. Inhibition of JNK potentiated STI571-induced cell death in melanoma B16F0 cells

Expressions of MAPKs, including ERK, JNK, p38, and AKT protein phosphorylation, in STI571-treated B16F0 cells were examined by Western blotting using specific antibodies. As illustrated in Fig. 5A, increases in phosphorylated JNK and p38, but not ERK or AKT, protein levels were detected in STI571-treated B16F0 cells. However, no significant change in total MAPKs or AKT protein was identified. Furthermore, pharmacological inhibitors, including SB203580 (SB) for p38 and SP600125 (SP) for JNK, were used to investigate the roles of JNK and p38 activation in STI571-induced cell death in melanoma B16F0 cells. Data of the MTT assay indicated that SP addition significantly increased STI571-induced cytotoxicity in B16F0 cells, however, less significant enhancement of p38 inhibitor SB203580 on STI571-induced cytotoxicity in B16F0 cells was observed (Fig. 5B). Examination of caspase 3 and PARP protein cleavage in STI571-treated cells with SB or SP addition showed that SP possessed an inductive ability to enhance

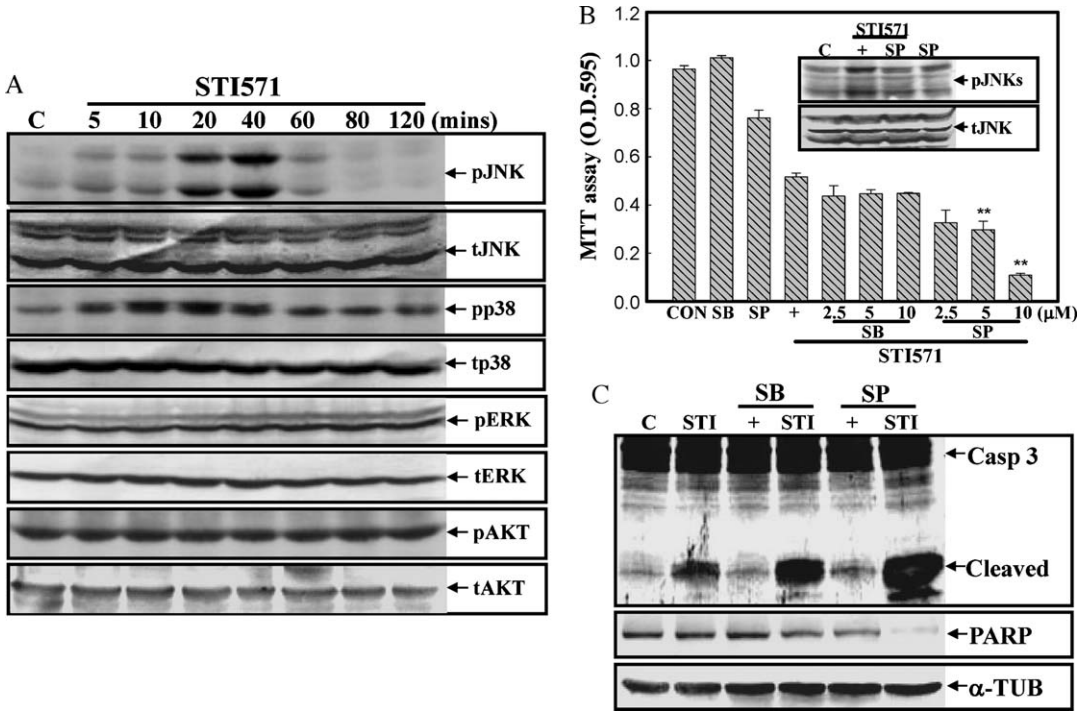

Fig. 5. Activation of JNK and p38 kinase in STI571-treated B16F0 cells. (A) Induction of JNK and p38, but not ERK or AKT protein phosphorylation by STI571 (STI) in B16F0 cells. Cells were treated with STI571 (20 μM) for different times, and the expressions of phosphorylated and total indicated proteins including JNK, p38, ERK, and AKT were detected by Western blotting using specific antibodies. (B) Effects of p38 inhibitor SB203580 (SB) and JNK inhibitor SP600125 (SP) on the viability of STI-treated B16F0 cells. Cells were treated with indicated concentrations of SB or SP for 30 min followed by STI (20 μM) treatment for an additional 24 h. Viability of cells under different treatments was evaluated by MTT assay. SP (10 μM) reduction of phospho-JNK protein expression in STI (20 μM)-treated B16F0 cells was detected by Western blotting. (C) Effects of SB and SP on STI-induced caspase 3 and PARP protein expression in B16F0 cells. Cells were treated with SB or SP (10 μM) for 30 min with or without STI571 (20 μM) treatment for an additional 24 h, and expression of caspase 3, PARP, and α-tubulin protein was examined by Western blotting. Data are expressed as the mean ± SE from three independent experiments. $^{**}p < 0.01$ denotes a significant difference compared to the STI571 (STI)-treated group by Student's *t*-test. Data of Western blotting and morphological observations have been repeated independently at least three times, and similar results were obtained.

caspase 3 and PARP protein cleavage elicited by STI571 in melanoma cells B16F0 (Fig. 5C).

4. Discussion

The goal of this study was to determine whether STI571-induced apoptosis occurred through ROS production in melanoma B16F0 cells. We found that STI571 reduced the viability of B16F0 cells through increases of apoptosis induction and ROS production. STI571-induced apoptotic events, including loss of the mitochondrial membrane potential, DNA ladder formation, and caspase activation, were inhibited by adding the antioxidant, NAC, and the NADPH oxidase inhibitor, DPI, to B16F0 cells. Induction of JNK and p38 protein phosphorylation by STI571 was identified, and the addition of the JNK inhibitor, SP600125, enhanced apoptosis elicited by STI571 in B16F0 cells. ROS-dependent apoptosis elicited by STI571 thorough disrupting mitochondrial functions was first demonstrated in melanoma B16F0 cells herein.

Apoptosis induced by STI571 was identified in several cells. Gordon and Fisher reported STI571-induced apoptosis in GIST cells through upregulation of proapoptotic BIM protein expression [23]. Biswas et al. indicated that STI571 induced apoptosis in retinal ganglion RGC-5 cells through inhibiting PDGF-induced PI3K/Akt survival signaling [24]. Additionally, a recent study indicated that STI571 induced growth arrest at a lower concentration (1–10 μM) and apoptosis at high concentrations (20, 30 μM) in glioblastoma cells [25]. Data of the present study which are consistent with those of previous studies showed that STI571 at doses of 10 and 20 μM induced apoptosis in melanoma B16F0 cells accompanied by stimulation of DNA ladders, and caspase 3 and PARP protein cleavage. Decreases in the mitochondrial membrane potential were detected in STI571-treated B16F0 cells via $DiOC_6$ staining in accordance with stimulation of caspase 9 protein cleavage and Cyt c protein translocation from mitochondria to the cytosol. This suggests that STI571-induced melanoma cell apoptosis is mediated in a mitochondrion-dependent manner.

There are conflicting data in the literature regarding the effects of ROS on apoptosis and the viability of different cancer cells including melanoma [26]. Dunning et al. indicated that ROS inhibited hepatic stellate cells (HSC) proliferation and promoted HSC death in vitro [27]. With ultraviolet (UV) B irradiation, production of ROS to induce G1 arrest and apoptosis was identified in cultured dermal fibroblasts [28]. However, treatment with H_2O_2 or UVB irradiation also significantly inhibited the induction of apoptosis in H_2O_2-sensitive, but not -resistant, cells [29]. Although both apoptotic and antiapoptotic effects of ROS in different in vitro models were reported, the role of ROS in STI571-induced apoptosis in melanoma cells is still undefined. In the present study, increased intracellular peroxide by STI571 was detected, and STI571-induced apoptotic events such as DNA ladders and caspase activation were prevented by the ROS scavenger, NAC. Additionally, application of the NADPH oxidase inhibitor, DPI, protected melanoma cells from STI571-induced apoptosis with decreased intracellular peroxide levels elicited by STI571 in B16F0 cells. ROS-dependent apoptosis was demonstrated at least in part to occur via activation of NADPH oxidase in STI571-treated melanoma cells.

Activation of MAPKs including ERKs, JNKs, and p38 MAPKs led to pro-growth, transformation, and apoptosis that appears to be critical to the pathogenesis of many malignancies [30]. Studies demonstrated that activation of the MAPK pathway was involved in facilitating chemotherapy resistance, and inducing resistance of tumor cells to apoptosis [31]. However, JNKs and p38 activation

has been shown to contribute to dual effects in pro- and anti-apoptosis [32,33]. Alexaki et al. indicated that JNK inhibition enhanced apoptosis of human melanoma cells, and Tsuchiya et al. reported that p38 inhibitor FR167653 induced apoptosis in human colon cancer cells [34,35]. In the present study, STI571 treatment stimulated the expressions of JNK and p38 protein phosphorylation in melanoma B16F0 cells, and application of the JNK inhibitor SP600125 enhanced the cytotoxic effects elicited by STI571. However, less significant enhancement of p38 inhibitor SB203580 on STI571-induced cytotoxicity in B16F0 cells was observed. Evidence of combined therapy on melanoma using JNK inhibitors and STI571 was provided for further investigation.

STI571 has been shown to effectively block activities of multiple tyrosine kinases such as c-Kit, PDGF-R, and Abl, however, the relationship between ROS production and tyrosine kinases inhibition by STI571 is still unclear. Several previous studies have shown that STI571 at the concentrations less than 5 μM effectively suppressed tyrosine kinases phosphorylation in different cells [36–38], whereas the applied concentration of STI571 to induced ROS production and apoptosis induction of melanoma cells B16F0 in the present study should reach to 20 μM, much higher than that for tyrosine kinases inhibition. It indicated that ROS production might not be attributed to tyrosine kinase receptors inhibition of STI571 in melanoma cells. Similarly, Yu et al. reported that STI571 at the concentration less than 5 μM interrupted cytoprotective MAPK activation response in human myeloid leukemia cells [39]. In our present study, a higher concentration (20 μM) of STI571 induced JNK and p38 protein phosphorylation in according with elevating ROS production in melanoma cells B16F0. Besides, nilotinib, a new generation of tyrosine kinase inhibitor, effectively induced ROS production with decreased viability of melanoma B16F0 cells. It suggested that higher concentrations of STI571 and its related compounds such as nilotinib possessed ability to stimulate JNK and p38 protein phosphorylation mediated by elevating ROS production in melanoma cells.

In summary, our study suggests an ROS-dependent apoptosis mechanism in STI571-treated melanoma cells. STI571-induced apoptosis was mediated by disrupting the mitochondrial membrane potential, releasing Cyt c protein, and activating caspase 9. Additionally, activations of JNK and p38 by STI571 were detected in melanoma cells, and the apoptotic effects of STI571 against melanoma cells were enhanced by adding the JNK inhibitor, SP600125. The combination of JNK inhibitors with STI571 or other tyrosine kinase inhibitors for treating melanomas is suggested for further in vivo studies.

Acknowledgements

This study was supported by the National Science Council of Taiwan (NSC96-2320-B-038-031-MY3 and 98-2320-B-038-002-MY3), and Taipei Medical University – Chi Mei Hospital (99CM-TMU-06).

References

[1] Cohen C, Zavala-Pompa A, Sequeira JH, Shoji M, Sexton DG, Cotsonis G, et al. Mitogen-actived protein kinase activation is an early event in melanoma progression. Clin Cancer Res 2002;8:3728–33.
[2] Meier F, Busch S, Lasithiotakis K, Kulms D, Garbe C, Maczey E, et al. Combined targeting of MAPK and AKT signaling pathways is a promising strategy for melanoma treatment. Br J Dermatol 2007;156:1204–13.
[3] Smalley KS, Haass NK, Brafford PA, Lioni M, Flaherty KT, Herlyn M. Multiple signaling pathways must be targeted to overcome drug resistance in cell lines derived from melanoma metastases. Mol Cancer Ther 2006;5:1136–44.
[4] Hu WP, Yu HS, Sung PJ, Tsai FY, Shen YK, Chang LS, et al. DC-81-indole conjugate agent induces mitochondria mediated apoptosis in human melanoma A375 cells. Chem Res Toxicol 2007;20:905–12.
[5] Doudican N, Rodriguez A, Osman I, Orlow SJ. Mebendazole induces apoptosis via Bcl-2 inactivation in chemoresistant melanoma cells. Mol Cancer Res 2008;8:1308–15.
[6] Yang J, Liu X, Bhalla K, Kim CN, Ibrado AM, Cai J, et al. Prevention of apoptosis by Bcl-2: release of cytochrome c from mitochondria blocked. Science 1997;275(5303):1129–32.
[7] Chandra J, Hackbarth J, Le S, Loegering D, Bone N, Bruzek LM, et al. Involvement of reactive oxygen species in adaphostin-induced cytotoxicity in human leukemia cells. Blood 2003;102:4512–9.
[8] Hervouet E, Simonnet H, Godinot C. Mitochondria and reactive oxygen species in renal cancer. Biochemistry 2007;89:1080–8.
[9] Galluzzi L, Larochette N, Zamzami N, Kroemer G. Mitochondria as therapeutic targets for cancer chemotherapy. Oncogene 2006;25:4812–30.
[10] Yi-Fen Wang YF, Chen CY, Chung SF, Chiou YH, Lo HR. Involvement of oxidative stress and caspase activation in paclitaxel-induced apoptosis of primary effusion lymphoma cells. Cancer Chemother Pharmacol 2004;54:322–30.
[11] Bragado P, Armesilla A, Silva A, Porras A. Apoptosis by cisplatin requires p53 mediated p38 alpha MAPK activation through ROS generation. Apoptosis 2007;12:1733–42.
[12] Tsang WP, Chau SPY, Kong SK, Fung KP, Kwok TT. Reactive oxygen species mediate doxorubicin induced p53-independent apoptosis. Life Sci 2003;73:2047–58.
[13] Wu WS, Wu JR, Hu CT. Signal cross talks for sustained MAPK activation and cell migration: the potential role of reactive oxygen species. Cancer Metastasis Rev 2008;27:303–14.
[14] Martindale JL, Holbrook NJ. Cellular response to oxidative stress: signaling for suicide and survival. J Cell Physiol 2002;192:1–15.
[15] Meyskens Jr FL, Farmer P, Fruehauf JP. Redox regulation in human melanocytes and melanoma. Pigment Cell Res 2001;14:148–54.
[16] Buchdunger E, Cioffi CL, Law N, Stover D, Ohno-Jones S, Druker BJ, et al. Abl protein-tyrosine kinase inhibitor STI571 inhibits in vitro signal transduction mediated by c-Kit and platelet-derived growth factor receptors. J Pharm Exp Ther 2000;295:139–45.
[17] Schindler T, Bornmann W, Pellicena P, Miller WT, Clarkson B, Kuriyan J. Structural mechanism for STI-571 inhibition of abelson tyrosine kinase. Science 2000;289:1938–42.
[18] David A, Tuveson DA, Willis NA, Jacks T, Griffin JD, Singer S, et al. STI571 inactivation of the gastrointestinal stromal tumor c-KIT oncoprotein: biological and clinical implications. Oncogene 2001;20:5054–8.
[19] Taira Maekawa T, Eishi Ashihara E, Kimura S. The Bcr-Abl tyrosine kinase inhibitor imatinib and promising new agents against Philadelphia chromosome-positive leukemias. Int J Clin Oncol 2007;12:327–40.
[20] Ogawa Y, Kawamura T, Furuhashi M, Tsukamoto K, Shimada S. Improving chemotherapeutic drug penetration in melanoma by imatinib mesylate. J Dermatol Sci 2008;51:190–9.
[21] Uziel O, Fenig E, Nordenberg J, Beery E, Reshef H, Sandbank J, et al. Imatinib mesylate (Gleevec) downregulates telomerase activity and inhibits proliferation in telomerase-expressing cell lines. Br J Cancer 2005;92:1881–91.
[22] Chow JM, Lin HY, Shen SC, Wu MS, Lin CW, et al. Zinc protoporphyrin inhibition of lipopolysaccharide-, lipoteichoic acid-, and peptidoglycan-induced nitric oxide production through stimulating iNOS protein ubiquitination. Toxciol Appl Pharmacol 2009;237:357–65.
[23] Gordon PM, David E, Fisher DE. Role for the proapoptotic factor BIM in mediating imatinib-induced apoptosis in a c-KIT-dependent gastrointestinal stromal tumor cell line. J Biol Chem 2010;285:14109–14.
[24] Biswas SK, Zhao Y, Sandirasegarane L. Imatinib induces apoptosis by inhibiting PDGF- but not insulin-induced PI 3-kinase/Akt survival signaling in RGC-5 retinal ganglion cells. Mol Vision 2009;15:1599–610.
[25] Ranza E, Mazzini G, Facoetti A, Nano R. In-vitro effects of the tyrosine kinase inhibitor imatinib on glioblastoma cell proliferation. J Neuro-Oncol 2010;96:349–57.
[26] Wittgen HGM, van Kempen LCLT. Reactive oxygen species in melanoma and its therapeutic implications. Melanoma Res 2007;17:400–9.
[27] Dunning S, Hannivoort RA, de Boer JF, Buist-Homan M, Faber KN, Moshage H. Superoxide anions and hydrogen peroxide inhibit proliferation of activated rat stellate cells and induce different modes of cell death. Liver Int 2009;29:922–32.
[28] Straface E, Vona R, Ascione B, Matarrese P, Strudthoff T, Franconi F, et al. Single exposure of human fibroblasts (WI-38) to a sub-cytotoxic dose of UVB induces premature senescence. FEBS 2007;581:4342–8.
[29] Placzek M, Bprzybilla B, Kerkmann U, Gaube S, Gilbertz KP. Effect of ultraviolet (UV) A, UVB or ionizing radiation on the cell cycle of human melanoma cells. Br J Dermatol 2007;156:843–7.
[30] Wagner EF, Nebreda AR. Signal integration by JNK and p38 MAPK pathways in cancer development. Nat Rev Cancer 2009;9:537–49.
[31] Hocker TL, Singh MK, Tsao H. Melanoma genetics and therapeutic approaches in the 21st century: moving from the benchside to the bedside. J Invest Dermatol 2008;128:2575–95.
[32] Liu J, Lin A. Role of JNK activation in apoptosis: a double-edged sword. Cell Res 2005;15:36–42.
[33] Zarubin T, Han JH. Activation and signaling of the p38 MAP kinase pathway. Cell Res 2005;15:11–8.
[34] Alexaki V-I, Javelaud D, Mauviel A. JNK supports survival in melanoma cells by controlling cell cycle arrest and apoptosis. Pigment Cell Melanoma Res 2008;21:429–38.

[35] Tsuchiya T, Tsuno NH, Asakage M, Yamada J, Yoneyama S, Okaji Y, et al. Apoptosis induction by p38 MAPK inhibitor in human colon cancer cells. Hepato-Gastroenterol 2008;55:930–5.
[36] Deininger Michel WN, Druker BJ. Specific targeted therapy of chronic myelogenous leukemia with imatinib. Pharmacol Rev 2003;55:401–23.
[37] Yasuda A, Sawai H, Takahashi H, Ochi N, Matsuo Y, Funahashi H, et al. The stem cell factor/c-*kit* receptor pathway enhances proliferation and invasion of pancreatic cancer cells. Mol Cancer 2006;5:46–56.
[38] Kumar S, Mishra N, Raina D, Saxena S, Kufe D. Abrogation of the cell death response to oxidative stress by the c-Abl tyrosine kinase inhibitor STI571. Mol Pharmacol 2003;63:276–82.
[39] Yu C, Krystal G, Varticovksi L, McKinstry R, Rahmani M, Dent P, et al. Pharmacologic mitogen-activated protein/extracellular signal-regulated kinase kinase/mitogen-activated protein kinase inhibitors interact synergistically with STI571 to induce apoptosis in Bcr/Abl-expressing human leukemia cells. Cancer Res 2002;62. 188-99.